Deliverable Number:	D 8.19
Deliverable Title:	**Validation of the measurements by Monte Carlo Simulation**
Delivery date:	Month 48
Leading beneficiary:	
Dissemination level:	Public
Status:	version 1
Authors:	Miguel Magán, ESS-Bilbao
	Octavio González, ESS-Bilbao
Project number:	654000
Project acronym:	SINE2020
Project title:	Worldclass Science and Innovation with Neutrons in Europe 2020
Starting date:	1st of October 2015
Duration:	48 months
Call identifier:	H2020-INFRADEV-2014-2015
Funding scheme:	Combination of CP & CSA – Integrating Activities

This project has received funding from the European Union's Horizon 2020 research and innovation programme under grant agreement No 654000

Abstract

In previous deliverable D8.5, a database of neutron transmission through a number of materials was created. Here, we make an example of how to employ said database to a shielding sizing and material choice. In this particular case, the Chopper Pit of the MIRACLES BeamLine in ESS[1] is used. The neutron flux and spectrum resulting from the interaction of the beam with the closed chopper is used as an input, and different configurations are calculated and compared, with a brief discussion about the calculation times and the possibilities this methodology opens.

Acknowledgements

This work was made possible thanks to both the experimental campaign performed at ChipIR by Uwe Filges (PSI), and the model of the same instrument provided by Steven Lilley (RAL). Fruitful discussion with Masako Yamada (PSI) are gratefully acknowledged.

1 Input on MIRACLES from private communication with Paula la Luna, ESS-Bilbao

Introduction

Neutron shielding in any complex geometry in general, and in beamlines in particular is a computational heavy task, that requiring CPU times in the order of thousands of CPU-hours per case studied. If studying a variety of shielding configurations, specially materials, there is also a significant personal work required. Modification of models in typical Monte Carlo codes like MCNP are also remarkably error-prone, which, in turn, typically lead to more corrections and more worktime used up. For this reason, usually very few configurations are tried out, and the modifications are kept as simple as possible.

For this reason, a complementary method to explore new shielding configurations, is of interest for design. This method is focused on speed and ease of calculation, even if the results can only be taken comparatively. Previously, in D8.3, a transmission factor library was compiled for a number of materials. The idea behind those transmission factors is that, for a monoenergetic incident neutron beam with intensity Φ , and energy E_0 the output spectrum can be defined as $\Phi'(E_i)=A(Ei,E_0)$, where $A(E_i,E_0)$ is the transmission factor corresponding to these energies. We can thus arrange those factors in a square matrix A, so that, for any entering spectrum, we can calculate the outlet spectrum as: $\Phi'(E)=A\cdot\Phi(E)$. This calculation is effectively immediate on any personal computer, thus allowing the shielding designer to try out as many configurations as he wishes without any access to High Performance Computer whatsoever.

As noted before, the results obtained using this method are only a first order approximation, and thus a full calculation will still be needed. Nevertheless, we believe this method can help the designers to quickly identify design alternatives, and then decide whether a full calculation is worth exploring or not.

In this work, we have tried to apply this method as well as traditional Monte Carlo calculation to the ChipIr instrument of the ISIS Second Target Station (ISIS-TS2). [2]. This results in a 3-way comparison, and the results are discussed.

2 C. Frost, et al. “A new dedicated neutron facility for accelerated SEE testing at the ISIS facility." Reliability Physics Symposium, 2009 IEEE International. IEEE, 2009.

N2 mineral cast transmission matrix

For this experiment, a custom-made mineral cast was made by PSI. As this material, being experimental, is not standardized and was not in the original D8.3 material list, the transmission values must be calculated. Table reflects the MCNP composition card used to simulate said material, and the transmission values are included as an annex. Remarkably, this material has very low transmission for any neutrons under 1 eV (below 1e-7). The full results are available as Annex 1.

Element	% Wgt abundance
Hydrogen (protium)	5
Carbon (Natural)	26
Oxygen-16	23.25
Magnesium (Natural)	0.7
Aluminum-27	2.3
Silicon (Natural)	38
Iron (Natural)	2
Nickel (Natural)	0.4
Boron-10	0.47
Boron-11	1.88

See D8.5 for information about methodology.

ChipIr MCNP Model

A initial ISIS-TS2 model featuring the ChipIr instrument line was provided for calculation. Figure **Error! Reference source not found.** shows an overall view of the model, and Figure **Error! Reference source not found.** gives a more detailed look of the experimental area.

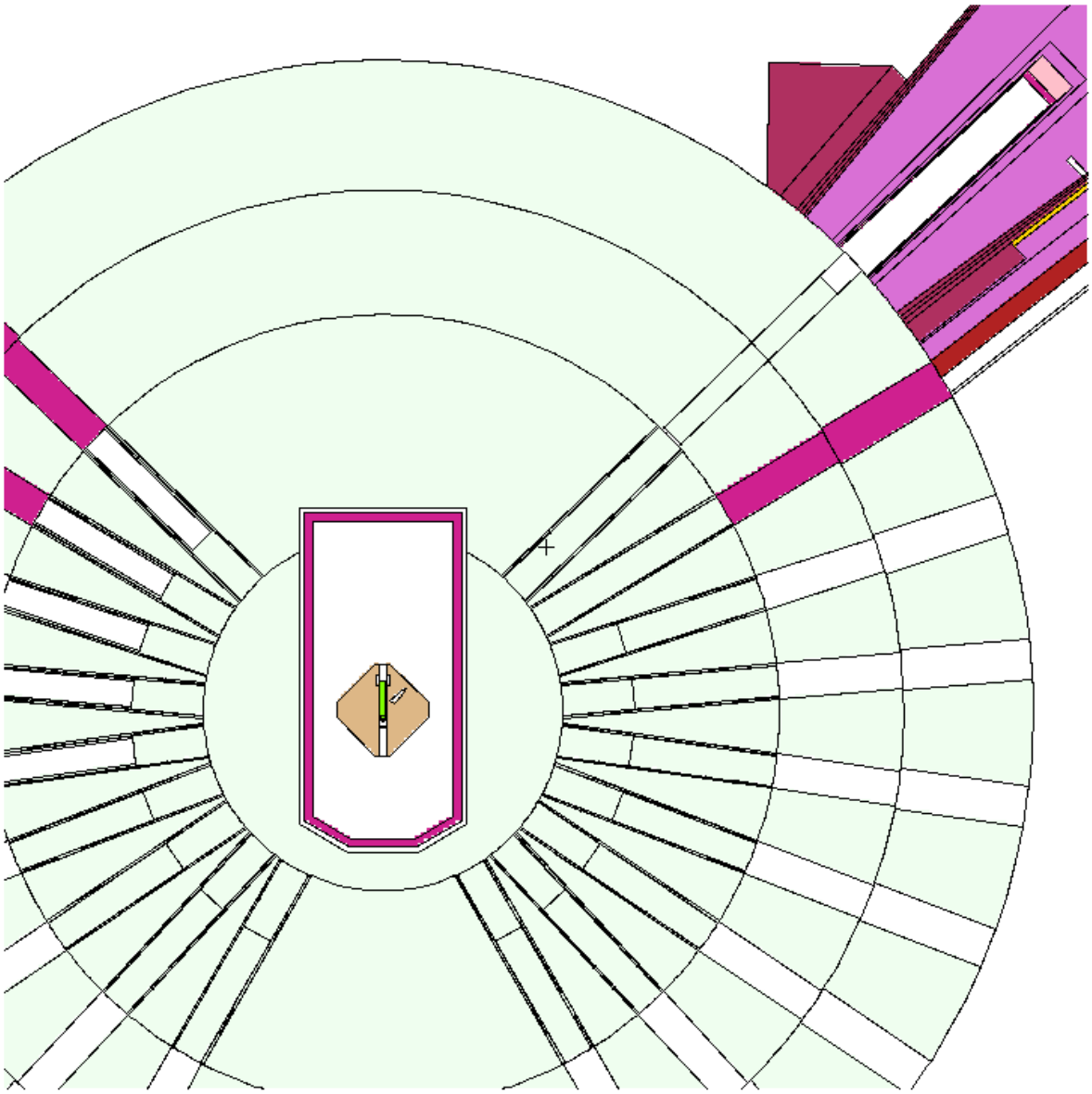

Figure 1: General view of the ISIS-TS2 model

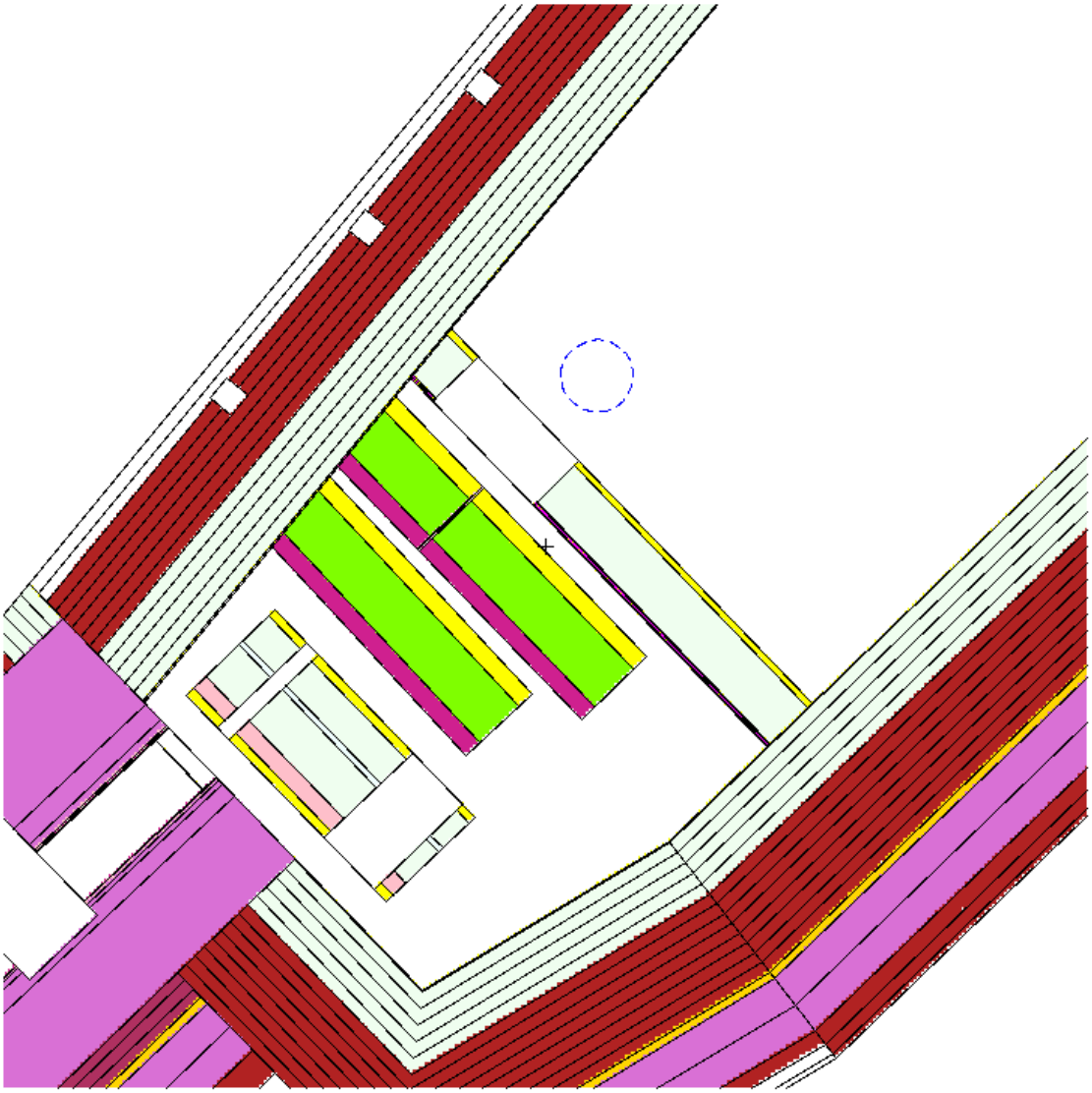

Figure 2: Overview of the ChipIr experimental area (original model)

This model was generated with CombLayer. Since we lack access to the source that generated it, we performed a few modifications to it to better reflect our conditions:

- The drum was substituted by transformed surfaces in order to allow easy rotation. Then, it was rotated to use the maximum aperture, as it was the one used in the experimental campaign.
- The horizontal and vertical jaws were adjusted to reflect different apertures.
- The point detector and tallies were modified to match the sample area, and to feature an energy binning useful for our purposes.

Figure 3 represents the result.

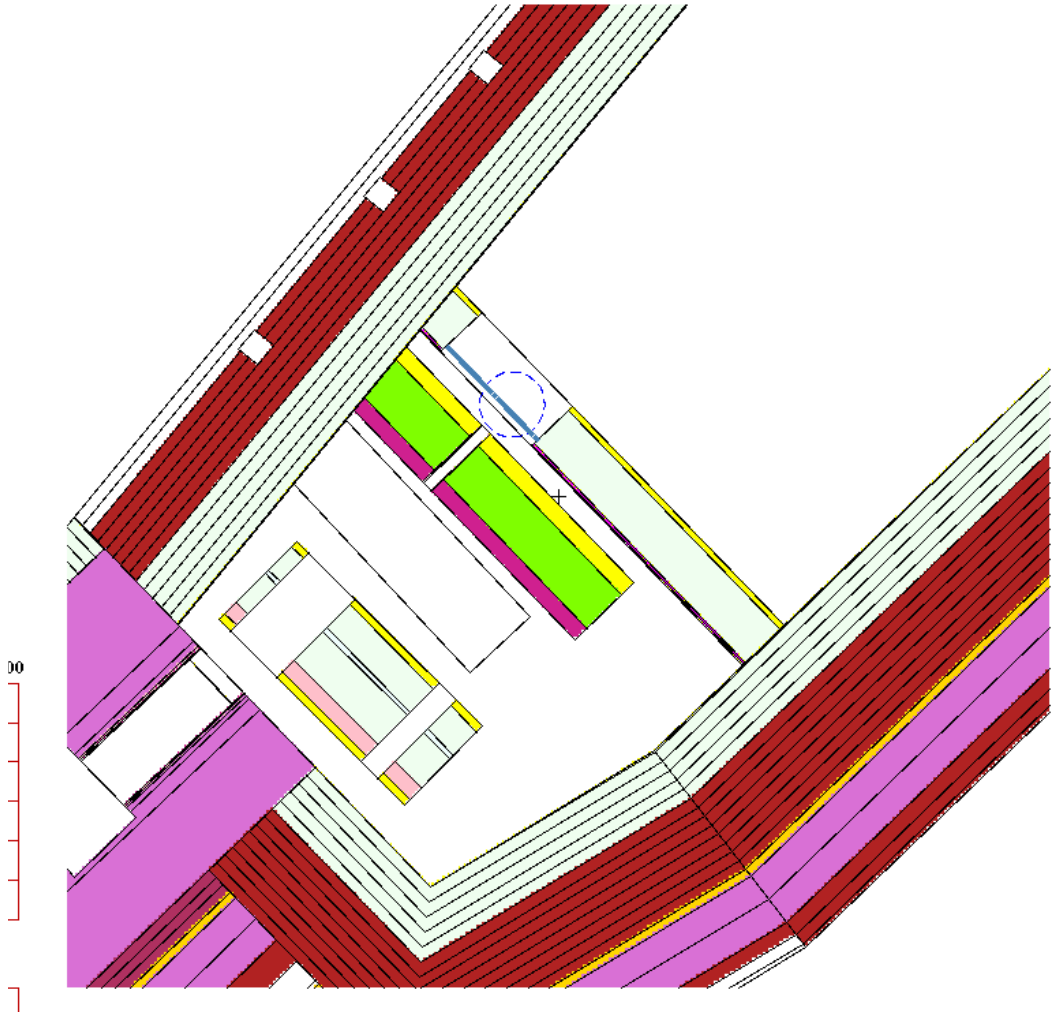

Figure 3: Overview of the Chipir experimental area with modified tallies and drum

A Global Variance Reduction Weight Window was generated for this model, using a MAGIC method[3]. The minimum importance value chosen was 1E-5,

3 Davis, Andrew Alexander and Andrew Turner. "APPLICATION OF NOVEL GLOBAL VARIANCE REDUCTION METHODS TO FUSION RADIATION TRANSPORT PROBLEMS." (2011).

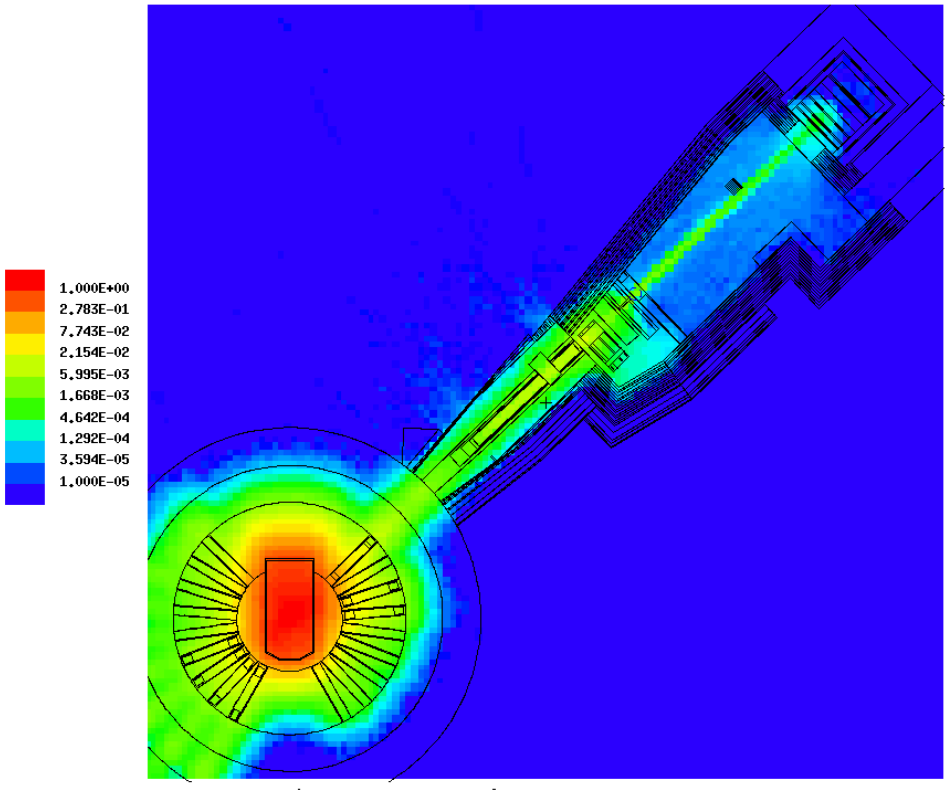

Figure 4: Weight window used for calculations

As an initial check to the model and variance reduction, the jaws opening was set to 70x70mm, and the spectrum in the point detector >0.1MeV was calculated and compared to known data [4]. The result, normalized to 5E+06 n/cm^2s^{-1} measured over 10 MeV, is plotted in Figure 5 on the right, with the comparison with reference 4 to the left .

4 Carlo Cazzaniga and Christopher D. Frost, IOP Conf. Series: Journal of Physics: Conf. Series 1021 (2018) 012037

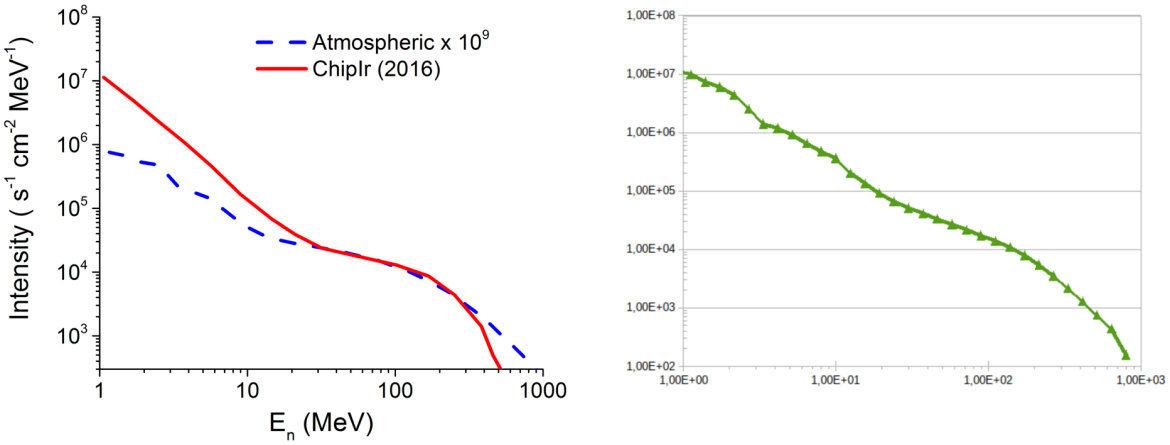

Figure 5: Measured spectrum at ChipIr from Reference 4 (left) and results from Monte Carlo model (right)

The results show reasonable agreement between both datasets. At the highest energies, near incident proton energy, the Monte Carlo simulation overestimate the spectrum somewhat, as an effect of using point detectors, which do not acccurately describe the anisotropy of the physics at those energies. This result shows that the model is a good description of the actual instrument.

Incident 10x10mm beam

As the experimental campaign was performed using this aperture, we first modified the jaws until the beam shape matched the 10x10mm beam. This determines the incident beam on the sample, and serves as a comparison to the experimental data. A mesh tally was set up with 1mm mesh size to track the results, and a separate run was used for the fast neutrons, using energy cutoff to accelerate the calculations and improve statistic. Figure 6 shows the incident beam for the three energy groups defined in Table 3.

Energy group	**Min energy**	**Max energy**
Thermal	1 meV	400 meV
Epithermal	400 meV	800 keV
Fast	800 keV	800 MeV

Table 3: Neutron energy groups

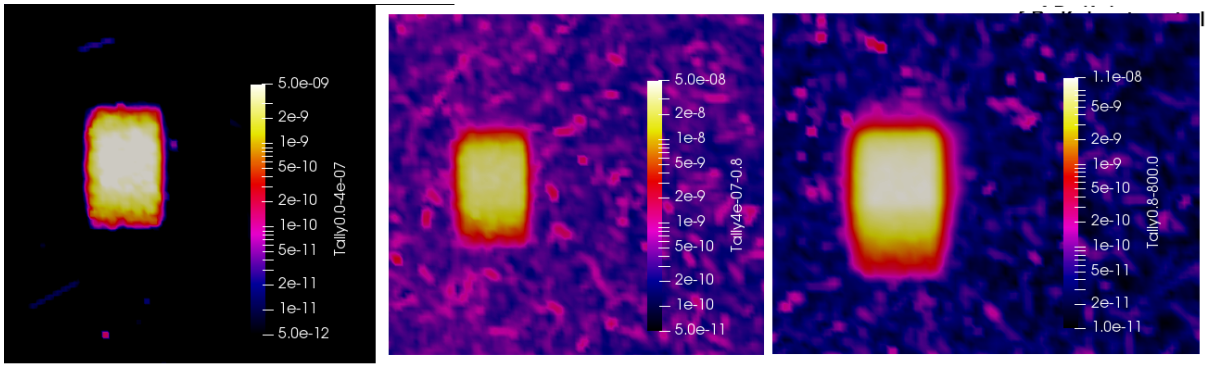

Figure 6: Incident beam for Thermal (left) Epithermal (mid) and fast (right) neutrons.

A few conclusions can be derived from these results and their comparisons with the incident beams from the experimental campaign:

- The shape of the beam seems slightly taller and less rounded than the experiments. This is likely a result of the adjustment of the jaws.
- The halo around the beam is clearly visible but significantly smaller in the simulations. Placement of the samples in the model and in reality, could influence this result. Importantly, the simulations agree with the experiment in that the relative size of the halo increases with the neutron energy.
- **While the simulation suffers from significant noise in the statistic, it successfully shows that the background around the beam is insignificant for thermal neutrons, and slightly higher from epithermal than from fast neutrons.**

Overall, and especially considering the limitations and simplifications used in the geometry, the Monte Carlo calculation achieve a rather positive approximation to the experimental measures.

Transmitted beam: Monte Carlo results

With the incident beam calculated, we proceeded to insert a block of the N2 mineral cast, 80mm wide, 80 mm thick and 120mm tall. The block was placed to in the trajectory of the beam, and the mesh tally was relocated to be directly behind it. The density of the cast was set to 2.4g/cc. As with the incident beam case, the fast neutrons were set up in a separate run to take advantage of energy cut-off.

Figure 7 shows the transmitted neutrons, in the same colour-scale as the corresponding incident beams. The mineral cast block is overlaid in the plots. Notice that in these simulations, incident beam hits the block roughly in the middle, while the experiments had the beam impinging rather close to the border, causing some differences in the shape of the beams that are rather intuitively understood.

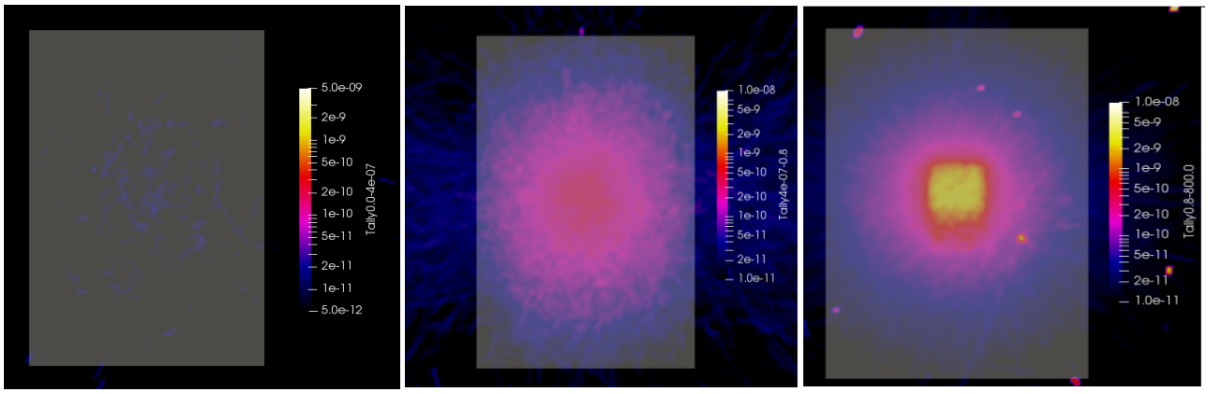

Figure 7: Transmitted beam for thermal, epithermal, and fast neutrons

In the case of thermal neutrons, the transmission is very low, causing the results to be barely detectable. This is, nevertheless, consistent with the results of the experimental campaign, where the transmission was 0.02 when measured in ChipIr and below 0.01 when measured in the Beamline for neutron Optics and other Approaches at the Paul Scherrer Institut (BOA-PSI). For the Epithermal and fast beam, the beam is attenuated and scattered, more so in the case of epithermal neutrons. This is qualitatively as expected, but the quantitative analysis is better done by calculating the transmission.

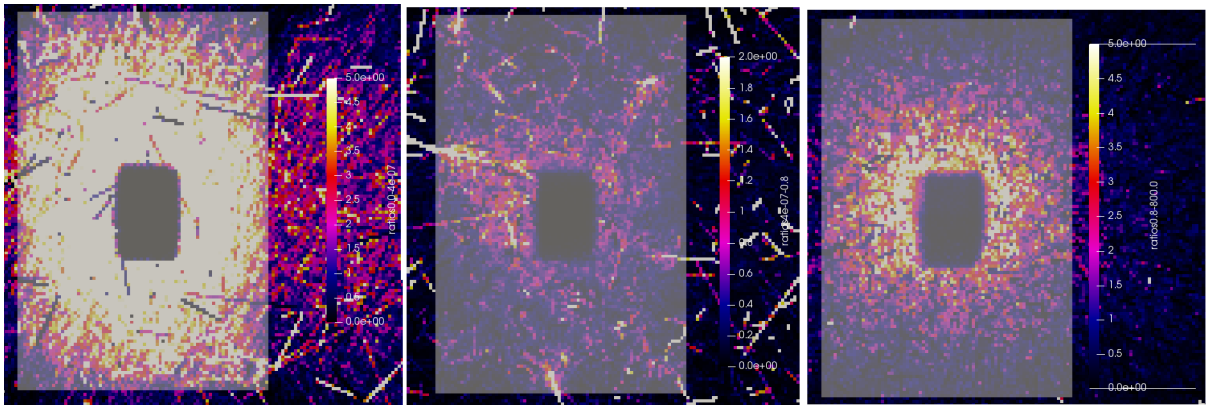

Figure 8: Figure 8: Transmission ratio for thermal, epithermal and fast neutrons.

Figure 8 shows the results of said ratios. Clearly, the definition is insufficient for such a high resolution calculation, with a lot of high weight tracks generating noise and . The beam footprint is very visible for all spectrum, much more so than in the experimentation. Overall, the results call into question wether the methodology in the experiment and the calculation are comparable.

Global transmission comparison between experimental, Monte Carlo, and transmission matrix method.

Finally, the overall transmission, defined as the overall flux, defined as the ratio of the fluxes with and without the sample in a 20x20cm centered in the beam, can be calculated in the Monte Carlo method. This result is compared with the experimental data provided, and with the application of the transmission matrix using the laminate shielding concept. Table 4 shows the results.

	Thermal	**Epithermal**	**Fast**
Monte Carlo	0.036	0.343	0.605
Laminate Shielding (Transmission matrix)	0.0052	0.0496	0.2433
Experimental (ChipIR)	0.02	0.63	0.93
Experimental (BOA-PSI)	<0.01	<0.01	0.58

The table shows that there is a great discrepancy between all the data, even the different experimental ones. However, there is also a degree of agreement in the relative results for the energy ranges, specially between the Monte Carlo method and the ChipIr setup it simulates. It is also worth noting that, in the experiment, the beam hits the sample quite near its edge, increasing the transmission compared to the Monte Carlo setup where the beam is quite centered. This is not significant for thermal neutrons, where the mean free path is a few mm, but is for the epithermal and fast neutrons, with mean free paths of several cm.

Regarding the transmission matrix shielding, it must be noted that said calculations are built with a material-geometry of an infinite plate, an assumption that is quite far from what we have in the experiment, so it is entirely expected that the transmission ratios are far lower. An interesting test for future project would be to test this method with much wider plates, in order to have a setup more similar to said setup. Besides, the testing and comparison of different materials could prove whether or not the calculation methods can predict the differences between them, even if the absolute results are not accurate. Overall, these results show that in order to achieve a better agreement, both a longer a more dedicated experimental campaign and a greater simulation effort would be needed.

INCIDENT ENERGY	1000 MeV		100 MeV		10 MeV		3 MeV		1 MeV		
Energy bins (M	Transmittance	error	Energy bins (Mısmittance Fa	error	Energy bins (Mısmittance Fa	error	Energy bins (Mısmittance Fa	error	Energy bins (Mısmittance Fa	error	Ene
1,00E-09	4,20E-08	0,1543	1,00E-09	4,80E-08	0,1443	1,00E-09	8,70E-08	0,1072	1,00E-09	1,24E-07	0,0898	1,00E-09	9,50E-08	1,03E-01	
3,00E-09	4,39E-07	0,0477	3,00E-09	4,72E-07	0,046	3,00E-09	6,77E-07	0,0384	3,00E-09	1,12E-06	0,0299	3,00E-09	8,73E-07	3,38E-02	
1,00E-08	5,03E-06	0,0141	1,00E-08	5,30E-06	0,0137	1,00E-08	8,46E-06	0,0109	1,00E-08	1,23E-05	0,009	1,00E-08	1,01E-05	1,00E-02	
3,00E-08	3,75E-05	0,0052	3,00E-08	3,95E-05	0,005	3,00E-08	6,29E-05	0,004	3,00E-08	9,24E-05	0,0033	3,00E-08	7,48E-05	3,70E-03	
1,00E-07	2,11E-04	0,0022	1,00E-07	2,22E-04	0,0021	1,00E-07	3,52E-04	0,0017	1,00E-07	5,22E-04	0,0014	1,00E-07	4,24E-04	1,50E-03	
3,00E-07	4,82E-04	0,0014	3,00E-07	5,08E-04	0,0014	3,00E-07	8,08E-04	0,0011	3,00E-07	1,20E-03	0,0009	3,00E-07	9,77E-04	1,00E-03	
1,00E-06	9,76E-04	0,001	1,00E-06	1,03E-03	0,001	1,00E-06	1,62E-03	0,0008	1,00E-06	2,40E-03	0,0006	1,00E-06	1,95E-03	7,00E-04	
3,00E-06	1,36E-03	0,0009	3,00E-06	1,43E-03	0,0008	3,00E-06	2,27E-03	0,0007	3,00E-06	3,35E-03	0,0005	3,00E-06	2,68E-03	6,00E-04	
1,00E-05	1,97E-03	0,0007	1,00E-05	2,07E-03	0,0007	1,00E-05	3,28E-03	0,0006	1,00E-05	4,80E-03	0,0005	1,00E-05	3,75E-03	5,00E-04	
3,00E-05	2,14E-03	0,0007	3,00E-05	2,26E-03	0,0007	3,00E-05	3,56E-03	0,0005	3,00E-05	5,17E-03	0,0004	3,00E-05	3,92E-03	5,00E-04	
1,00E-04	2,63E-03	0,0006	1,00E-04	2,77E-03	0,0006	1,00E-04	4,37E-03	0,0005	1,00E-04	6,27E-03	0,0004	1,00E-04	4,57E-03	5,00E-04	
3,00E-04	2,60E-03	0,0006	3,00E-04	2,73E-03	0,0006	3,00E-04	4,31E-03	0,0005	3,00E-04	6,11E-03	0,0004	3,00E-04	4,25E-03	5,00E-04	
1,00E-03	3,03E-03	0,0006	1,00E-03	3,19E-03	0,0006	1,00E-03	5,01E-03	0,0004	1,00E-03	7,02E-03	0,0004	1,00E-03	4,65E-03	5,00E-04	
3,00E-03	2,95E-03	0,0006	3,00E-03	3,10E-03	0,0006	3,00E-03	4,86E-03	0,0005	3,00E-03	6,72E-03	0,0004	3,00E-03	4,21E-03	5,00E-04	
1,00E-02	3,49E-03	0,0005	1,00E-02	3,68E-03	0,0005	1,00E-02	5,76E-03	0,0004	1,00E-02	7,83E-03	0,0004	1,00E-02	4,62E-03	5,00E-04	
3,00E-02	3,67E-03	0,0005	3,00E-02	3,87E-03	0,0005	3,00E-02	6,04E-03	0,0004	3,00E-02	8,09E-03	0,0004	3,00E-02	4,48E-03	5,00E-04	
1,00E-01	5,32E-03	0,0004	1,00E-01	5,60E-03	0,0004	1,00E-01	8,74E-03	0,0003	1,00E-01	1,15E-02	0,0003	1,00E-01	6,01E-03	4,00E-04	
3,00E-01	7,92E-03	0,0004	3,00E-01	8,34E-03	0,0003	3,00E-01	1,29E-02	0,0003	3,00E-01	1,69E-02	0,0002	3,00E-01	8,17E-03	3,00E-04	
1,00E+00	1,80E-02	0,0002	1,00E+00	1,90E-02	0,0002	1,00E+00	2,95E-02	0,0002	1,00E+00	3,85E-02	0,0002	1,00E+00	1,99E-02	2,00E-04	
3,00E+00	3,05E-02	0,0002	3,00E+00	3,27E-02	0,0002	3,00E+00	6,07E-02	0,0001	3,00E+00	1,26E-01	0,0001				
1,00E+01	2,67E-02	0,0002	1,00E+01	3,18E-02	0,0002	1,00E+01	2,49E-01	0,0001							
3,00E+01	6,86E-03	0,0004	3,00E+01	1,73E-02	0,0002										
1,00E+02	5,67E-03	0,0004	1,00E+02	5,01E-01	0										
3,00E+02	1,16E-02	0,0003													
1,00E+03	5,16E-01	0													

	0,03 MeV		0.01 MeV		0.003 MeV		0.001 MeV		0.0003 MeV		
Energy bins (M	Transmittance	error	Energy bins (Mısmittance Fa	error	Energy bins (Mısmittance Fa	error	Energy bins (Mısmittance Fa	error	Energy bins (Mısmittance Fa	error	Ene
1,00E-09	1,30E-08	0,2774	1,00E-09	1,40E-08	0,2673	1,00E-09	8,00E-09	0,1118	1,00E-09	5,50E-09	0,1348	1,00E-09	2,92E-09	0,0828	
3,00E-09	1,48E-07	0,0822	3,00E-09	1,16E-07	0,0928	3,00E-09	7,70E-08	0,0360	3,00E-09	5,27E-08	0,0436	3,00E-09	2,71E-08	0,0272	
1,00E-08	2,05E-06	0,0221	1,00E-08	1,30E-06	0,0278	1,00E-08	8,76E-07	0,0107	1,00E-08	5,56E-07	0,0134	1,00E-08	3,13E-07	0,008	
3,00E-08	1,51E-05	0,0081	3,00E-08	1,03E-05	0,0099	3,00E-08	6,68E-06	0,0039	3,00E-08	4,22E-06	0,0049	3,00E-08	2,36E-06	0,0029	
1,00E-07	8,83E-05	0,0034	1,00E-07	6,03E-05	0,0041	1,00E-07	3,91E-05	0,0016	1,00E-07	2,50E-05	0,0020	1,00E-07	1,40E-05	0,0012	
3,00E-07	2,05E-04	0,0022	3,00E-07	1,39E-04	0,0027	3,00E-07	9,12E-05	0,0010	3,00E-07	5,86E-05	0,0013	3,00E-07	3,28E-05	0,0008	
1,00E-06	3,98E-04	0,0016	1,00E-06	2,70E-04	0,0019	1,00E-06	1,74E-04	0,0008	1,00E-06	1,11E-04	0,0010	1,00E-06	6,13E-05	0,0006	
3,00E-06	5,05E-04	0,0014	3,00E-06	3,36E-04	0,0017	3,00E-06	2,12E-04	0,0007	3,00E-06	1,31E-04	0,0009	3,00E-06	6,95E-05	0,0005	
1,00E-05	6,20E-04	0,0013	1,00E-05	3,95E-04	0,0016	1,00E-05	2,39E-04	0,0006	1,00E-05	1,39E-04	0,0008	1,00E-05	6,85E-05	0,0005	
3,00E-05	5,32E-04	0,0014	3,00E-05	3,19E-04	0,0018	3,00E-05	1,79E-04	0,0007	3,00E-05	9,59E-05	0,0010	3,00E-05	4,08E-05	0,0007	
1,00E-04	4,77E-04	0,0014	1,00E-04	2,63E-04	0,002	1,00E-04	1,32E-04	0,0009	1,00E-04	6,14E-05	0,0013	1,00E-04	2,03E-05	0,001	
3,00E-04	3,18E-04	0,0018	3,00E-04	1,55E-04	0,0025	3,00E-04	6,56E-05	0,0012	3,00E-04	2,37E-05	0,0021	3,00E-04	4,45E-06	0,0021	
1,00E-03	2,28E-04	0,0021	1,00E-03	9,24E-05	0,0033	1,00E-03	2,95E-05	0,0018	1,00E-03	6,40E-06	0,0040				
3,00E-03	1,19E-04	0,0029	3,00E-03	3,61E-05	0,0053	3,00E-03	6,38E-06	0,0040							
1,00E-02	6,32E-05	0,0040	1,00E-02	1,08E-05	0,0096										
3,00E-02	2,06E-05	0,0070													

	0.00001 meV		0.000003 MeV		0.000001 meV		0.0000003 MeV		0.0000001 meV		
	MINERAL CAST		MINERAL CAST		MINERAL CAST		MINERAL CAST		MINERAL CAST		
Energy bins (M	Transmittance	error	Energy bins (Mısmittance Fa	error	Energy bins (Mısmittance Fa	error	Energy bins (Mısmittance Fa	error	Energy bins (Mısmittance Fa	error	Ene
1,00E-09	1,82E-10	0,0733	1,00E-09	3,75E-11	0,0403	1,00E-09	4,70E-12	0,1140	1,00E-09	1,22E-13	0,3162	1,00E-09	1,22E-14	**0,5**	
3,00E-09	1,67E-09	0,0242	3,00E-09	3,28E-10	0,0136	3,00E-09	4,24E-11	0,0379	3,00E-09	1,33E-12	0,0958	3,00E-09	2,44E-14	0,3536	
1,00E-08	2,04E-08	0,0069	1,00E-08	3,91E-09	0,0040	1,00E-08	4,70E-10	0,0114	1,00E-08	1,64E-11	0,0274	1,00E-08	4,70E-13	0,0806	
3,00E-08	1,62E-07	0,0025	3,00E-08	3,14E-08	0,0014	3,00E-08	3,82E-09	0,0041	3,00E-08	1,44E-10	0,0093	3,00E-08	4,40E-12	0,0268	
1,00E-07	9,94E-07	0,0011	1,00E-07	2,00E-07	0,0006	1,00E-07	2,57E-08	0,0017	1,00E-07	1,05E-09	0,0036	1,00E-07	3,65E-11	0,0104	
3,00E-07	2,37E-06	0,0008	3,00E-07	4,81E-07	0,0005	3,00E-07	6,26E-08	0,0012	3,00E-07	2,54E-09	0,0027				
1,00E-06	4,04E-06	0,0007	1,00E-06	7,41E-07	0,0005	1,00E-06	7,40E-08	0,0013							
3,00E-06	3,41E-06	0,0009	3,00E-06	4,10E-07	0,0007										
1,00E-05	1,56E-06	0,0014													

ANNEX 1: Transmission calculations for mineral cast